

Suprachoroidally Delivered DNA Nanoparticles Transfect Retina and Retinal Pigment Epithelium/Choroid in Rabbits

Viral S. Kansara¹, Mark Cooper², Ozge Sesenoglu-Laird², Leroy Muya¹, Robert Moen², and Thomas A. Ciulla¹

¹ Clearside Biomedical, Inc., Alpharetta, GA, USA

² Copernicus Therapeutics, Inc., Cleveland, OH, USA

Correspondence: Thomas A. Ciulla, Clearside Biomedical, Inc., 900 Northpoint Parkway Suite 200, Alpharetta, GA 30005, USA. e-mail: thomas.ciulla@clearsidebio.com

Received: July 24, 2020

Accepted: October 16, 2020

Published: December 15, 2020

Keywords: suprachoroidal delivery; nonviral gene therapy; DNA nanoparticles; chorioretinal diseases

Citation: Kansara VS, Cooper M, Sesenoglu-Laird O, Muya L, Moen R, Ciulla TA. Suprachoroidally delivered DNA nanoparticles transfect retina and retinal pigment epithelium/choroid in rabbits. *Trans Vis Sci Tech.* 2020;9(13):21, <https://doi.org/10.1167/tvst.9.13.21>

Purpose: This study evaluated ocular tolerability and transfectability of nonviral DNA nanoparticles (DNPs) after microneedle-based suprachoroidal (SC) administration, in comparison to subretinal (SR) administration.

Methods: The DNPs consisted of a single copy of plasmid DNA with a polyubiquitin C/luciferase transcriptional cassette compacted with 10 kDa PEG-substituted lysine 30-mer peptides (CK30PEG10k). New Zealand White rabbits ($n = 4$ per group) received a unilateral SC injection (0.1 mL via a microneedle technique) of ellipsoid-shaped DNPs, rod-shaped DNPs, or saline (negative control). A cohort of rabbits ($n = 4$) also received a single unilateral SR injection (0.05 mL via a transvitreal approach) of rod-shaped DNPs. At day 7, luciferase activity was measured in the retina and retinal pigment epithelium (RPE)–choroid via bioluminescence assay. A cohort of rabbits received a SC injection of analogous DNPs to assess spread of DNP injectate in the suprachoroidal space (SCS) via optical coherent tomography and histology.

Results: Suprachoroidal injection of DNPs resulted in reversible opening of the SCS circumferentially and posteriorly and was generally well tolerated, with no significant ocular examination score changes, intraocular pressure abnormalities, or changes in electroretinography amplitudes on day 7 compared to the baseline. High luciferase activity was observed in the retina and RPE-choroid of eyes that received SC DNPs (rod and ellipsoid shape) and SR DNPs (rod shape) compared to controls. The mean luciferase activity in RPE-choroid and retina was comparable between SC and SR administrations. Transfection in the RPE-choroid was approximately 10-fold higher than in the retina after either SC or SR administration of DNPs.

Conclusions: Suprachoroidal and SR administration of DNPs resulted in comparable transfection of retina and RPE-choroid.

Translational Relevance: Suprachoroidal delivery of DNPs offers the potential to precisely target chorioretinal tissues while avoiding surgical risks associated with SR injection, and it may offer an office-based nonsurgical gene therapy option for the treatment of retinal diseases.

Introduction

Retinal gene therapy has gained significant momentum since the 2017 US Food and Drug Administration (FDA) approval of adeno-associated virus (AAV) vector-based gene therapy for patients with RPE65 mutation-associated inherited retinal dystrophy (IRD).¹ Gene augmentation clinical trials are

currently under way for other IRDs, such as achromatopsia, choroideremia, Stargardt disease, Usher syndrome, and X-linked retinitis pigmentosa.^{2–4} In addition to gene augmentation for IRDs, which addresses genetic mutations in native genes, an alternative strategy involves converting native cells into “biofactories,” producing and secreting nonnative therapeutic proteins to treat multifactorial acquired conditions, such as age-related macular degeneration

(AMD), diabetic retinopathy (DR), diabetic macular edema (DME), and geographic atrophy (GA).^{5–8}

DNA nanoparticles (DNPs) are a promising nonviral vector that may overcome some of the limitations of viral vector-based retinal gene therapy. Nonviral DNPs offer unique advantages over viral vectors. Their large cargo capacity (≥ 20 kbp) enables delivery of large genes that cannot be delivered via traditional AAV vectors.⁹ Unlike AAV vectors, nonviral DNPs incur reduced risk of immune response and consequently offer the potential for repeatable dosing. Additionally, in contrast to manufacturing challenges associated with AAV-based vectors, the manufacturing process of DNPs is simpler, not involving host cell lines, and is thus more readily scalable.¹⁰ DNPs composed of single molecules of DNA compacted with 10 kDa polyethylene glycol (PEG)-substituted lysine 30-mers (CK30PEG) have been shown to be safe and efficacious in a human clinical trial for cystic fibrosis, and they have been employed in preclinical studies in the lung, brain, and eye.^{11–15} PEG-substituted polylysine-based DNPs (10–25 nm) are taken up by both passive (pinocytosis) and active mechanisms (cell surface nucleolin).^{16–18} The safety, efficacy, and durability of these DNPs have been demonstrated after subretinal (SR) or intravitreal (IVT) administration in preclinical models of retinal diseases.^{13,19–22} Additionally, the potential for therapeutic application of DNPs has been emphasized by their ability to produce comparable reporter gene expression to AAVs.²³

Delivery of the vector to the target retinal tissue involves several potential approaches. Subretinal injection is a clinically used route of administration for retinal gene delivery with the FDA-approved gene therapy product. Several clinical trials employing SR administration are currently in progress for inherited and noninherited retinal diseases.²⁴ Subretinal delivery of genetic material to the retinal pigment epithelium (RPE) and/or photoreceptors involves pars plana vitrectomy (PPV), followed by retinotomy with subsequent injection of the vector into the SR space. This procedure assumes the risks of PPV, retinotomy, and temporary focal retinal detachment (in an already compromised retina). While SR delivery facilitates direct delivery of the genetic material to the affected cell layer, the delivered vectors show limited spread beyond the SR injection site, which may result in suboptimal therapy for peripheral retinal disorders. Therefore, less invasive administration procedures, such as intravitreal or suprachoroidal injection, with potential for fewer procedure-related complications, are being sought.

The success of intravitreally delivered AAV vector-based gene therapy is limited due to the potential immune and inflammatory response, as well as the

diminished bioavailability in the photoreceptor and RPE cells due to the presence of internal limiting membrane.^{25–27} Suprachoroidal (SC) injection is a noninvasive route of administration that offers targeted and compartmentalized delivery of therapeutic agents to the posterior segment of the eye.²⁸ Recently, successful gene transfer after a freehand SC injection of both viral vectors and nonviral nanoparticles was demonstrated preclinically.^{29,30} In our opinion, the freehand SC injection technique is difficult to reliably perform in the clinic. Microneedle-based SC injection of a pharmacotherapy has been validated in a phase III clinical trial,³¹ and this method applied to viral vector administration has potential to facilitate office-based gene therapy.^{32,33}

To our knowledge, ocular safety and retinal cell transfectability of DNPs after microneedle-based delivery to the suprachoroidal space (SCS) have not been assessed previously. We hypothesized that SC administration offers potential advantages over SR administration, such as minimally invasive injection procedure and potential to develop an office-based gene therapy. Therefore, the aim of this proof-of-concept study was to assess ocular tolerability and transfectability of DNPs via SC administration, an emerging route of administration, in comparison to well-established SR administration for retinal gene delivery.

Materials and Methods

Reporter Gene Plasmid Design

pEUL is a 5503-bp luciferase expression plasmid and comprises the polyubiquitin C promoter, cytomegalovirus (CMV) enhancer, CpG-depleted luciferase gene, SV40 polyA site, flanking β -globin and interferon- β S/MAR domains, and the zeomycin resistance gene. It is a derivative of the pUL plasmid with insertion of the CMV enhancer.¹¹

DNP Formulation Preparation

pEUL was compacted into DNPs using a 10-kDa PEG-substituted lysine 30-mer peptide (CK30PEG10k) as previously reported.^{11,34,35} Each DNP consists essentially of a single molecule of plasmid DNA. Rod-like and ellipsoid nanoparticles (NPs) were produced by varying the lysine counterion at the time of DNA compaction, with an acetate counterion producing rods and a trifluoroacetate counterion producing ellipsoids.⁹ The internal volume of these two shapes is equivalent and depends on

the partial specific volume of DNA and lysine.^{9,34} After compaction, DNPs were solvent exchanged in saline and concentrated to approximately 4 mg/mL DNA concentration. The formulations were stored refrigerated (2°C–8°C) until the day of dosing.

DNP Formulation Characterization

DNPs were evaluated with a panel of quality control tests to determine if these particles met all internal specifications, including being unimolecular with respect to DNA molecules per nanoparticle, colloidal stability without aggregation in saline, light-scattering criteria, size and shape parameters as determined by transmission electron microscopy, sedimentation criteria in charge neutrality, low endotoxin (<5 EU/mg), and osmolality parameters.^{14,34,35} Stability of compacted DNPs in physiologic saline was assayed via a DNP sedimentation quality control assay, as described previously by Liu et al.³⁴ Briefly, the DNP formulation was diluted with 5 M NaCl to achieve a final concentration of 150 mM and then spun at $3400 \times g$ for 1 minute at room temperature. The DNA concentration in supernatant was compared to the initial sample presedimentation. Each quality control assay had formal end-release specifications that had previously been reviewed by the FDA in the Copernicus IND for a cystic fibrosis clinical trial.¹²

In Vivo Experiments

Institutional Animal Care and Use Committee Compliance

All animal experiments were conducted in accordance with the Association for Research in Vision and Ophthalmology (ARVO) Statement for the Use of Animals in Ophthalmic and Vision Research and the guidelines of the Animal Care Committee of Keio University. The experimental protocols were approved by the Powered Research Institutional Animal Care and Use Committee (IACUC).

Animals, Housing, Environmental Conditions, and Diet

Rabbit is a commonly used species for ocular pharmacokinetics and ocular toxicology studies due to the size of their eyes that is suitable for the accurate and reliable delivery of test articles in the suprachoroidal space. Ocular pharmacokinetics and distribution of several biologics have been studied in rabbits.³⁶

New Zealand White (NZW) rabbits have been previously employed as a preclinical animal model for retinal gene delivery via suprachoroidal administration.³⁷ NZW rabbits (*Oryctolagus cuniculus*) from Covance (King of Prussia, PA, USA), 2 to 3 kg (aged 4–6 months), were housed in a stainless-steel cage, singly, under a 12-hour light/12-hour darkness photoperiod and at a temperature of $68^{\circ}\text{F} \pm 2^{\circ}\text{F}$.

Animal Health and Acclimation

Rabbits were acclimated to the study environment for at least 1 week prior to anesthesia. During acclimation and while on study, animals were evaluated for mortality and morbidity as well as general health, with special attention to the eyes. At the completion of the acclimation period, each rabbit was physically examined by a laboratory animal technician for determination of suitability for study participation. All rabbits were determined to be in good health and were released to the study.

Randomization and Study Identification

Rabbits were assigned to study groups according to SOPs. Specifically, rabbits were assigned to groups by a stratified randomization scheme designed to achieve averaged mean weight in each group. Each study animal was uniquely identified by corresponding cage card number and ear tagging.

Ocular Dosing

The injections were performed by an experienced veterinary ophthalmologist to the left eyes, and the right eyes were left undosed in each group.

For suprachoroidal injections, an eyelid speculum was placed, and saline (vehicle control) or luciferase rod-shaped or ellipsoid-shaped DNPs were administered (0.1 mL) into the SC space of the left eye ($n = 4$ rabbits per group) by an experienced veterinary ophthalmologist using a proprietary 30-gauge microneedle 700 μm in length (Clearside microinjector, Alpharetta, GA).

A cohort of rabbits ($n = 4$) also received a single unilateral (left eye) SR injection (0.05 mL via a transvitreal approach) of rod-shaped DNPs. For subretinal injection, the rabbit was placed under an operating microscope equipped with a BIOM 5 and SDI (Stereoscopic Diagonal Inverter) posterior segment imaging system (Oculus, Inc., Arlington, WA). The superior and temporal quadrants of the eye were used for placement of transscleral cannulas, which were inserted using a microvitreal 25-gauge self-sealing port

system (Alcon, Fort Worth, TX). The ports were angled toward the posterior pole of the globe to avoid lens damage. One port was used for insertion of a handheld fiber optic light source into the globe and the second for the subretinal cannula. The transscleral SR cannula with an extendable 41-gauge inner flexible injection cannula was placed through the port and the flexible cannula extended until the tip contacted the inner retinal surface. With the bore of the cannula in contact with the retina, the injection of fluid created a retinotomy. The luciferase rod-shaped DNPs were very slowly pushed through the cannula by a surgical assistant to create a SR bleb. Once the entire dose volume was administered, the injection device was removed, followed by removal of the self-sealing ports. A drop of antibiotic ophthalmic solution was applied following completion of dosing, and rabbits were allowed to recover normally from the procedure.

Ocular Tolerability Assessment

Ocular Examinations

A veterinary ophthalmologist performed complete ocular examinations using a slit-lamp biomicroscope and indirect ophthalmoscope to evaluate ocular surface morphology and anterior and posterior segment inflammation. All animals were examined prior to injection, to serve as a baseline, 24 hours postinjection and at harvest on day 7. The Hackett and McDonald³⁸ ocular grading system was used for scoring. Animals were not tranquilized for the examinations.

Tonometry

Intraocular pressure (IOP) was measured in both eyes prior to injections (baseline) and at day 1 and day 7 postinjection. The measurements were taken using a Tonovet probe (iCare Tonometer, Espoo, Finland) without use of topical anesthetic.

Electroretinography

Electroretinography (ERG) was conducted on both eyes of all rabbits at baseline and before euthanasia. All animals were dark adapted for at least 15 minutes prior to ERG. ERG was elicited by brief flashes at 0.33 Hz delivered with a mini-ganzfeld photostimulator (Roland Instruments, Wiesbaden, Germany) at maximal intensity. Twenty responses were amplified, filtered, and averaged (Retiport Electrophysiology Diagnostic Systems; Roland Instruments) for each animal. The response times and b-wave amplitudes were reported.

Optical Coherent Tomography/Infrared Imaging

A separate cohort of Dutch Belted rabbits ($n = 4$ rabbits, aged 4–6 months) underwent optical coherent tomography (OCT) to assess the spread of injectate (analogous DNPs) after SC injection. The OCT sessions were performed at baseline, on day 1, and 1 month (day 30 ± 2) after SC injection using a Heidelberg Spectralis OCT device (Heidelberg, Germany). OCT scans were performed in the superior, inferior, nasal, and temporal quadrants, as well as the posterior pole, with a 55° field of view using the high-resolution mode (signal quality, ≥ 24 dB) with a scan speed of 40,000 A-scans per second.

Histology

Eyes from a separate cohort of NZW rabbits ($n = 4/\text{group}$, aged 4–6 months) underwent histology assessment after a single unilateral (left eye) SC or SR injection of analogous DNPs (group 1, ellipsoid DNPs via SC injection; group 2, rod DNPs via SC injection; and group 3, rod DNPs via SR injection). Immediately following euthanasia on day 7, both eyes were enucleated and placed in Davidson's fixative overnight and then transferred to 70% ethanol. The eyes were trimmed and embedded in paraffin for sectioning. Sections were stained with hematoxylin and eosin.

Ocular Tissue Collection and Luciferase Activity Assay

One week after dosing and following the final examinations and procedures, animals ($n = 4$ per group) were euthanized with an overdose of sodium pentobarbital (Euthasol solution, Virbac, Inc., Fort Worth, TX). Immediately following euthanasia, both eyes were enucleated, fresh aqueous humor was collected to depressurize the eyes, and the globes were flash frozen. Retina and RPE-choroid were dissected from each eye while frozen and placed in preweighed tubes. The tubes were then weighed to determine the tissue weight and immediately placed on dry ice until transfer to a -80°C freezer. Frozen samples were stored at -80°C until overnight shipment on dry ice for further analysis. The ocular tissues were pulverized with a Qialyzer (Qiagen, Germantown, MD, USA) and luciferase enzyme activity measured using a Promega kit (Madison, WI, USA), as previously reported.³⁵

Statistical Analysis

All available data were used in the analysis, and no data were excluded for any reason. Results are expressed as mean \pm SD. Inferential statistics for IOP in the treated and untreated eyes were based on a

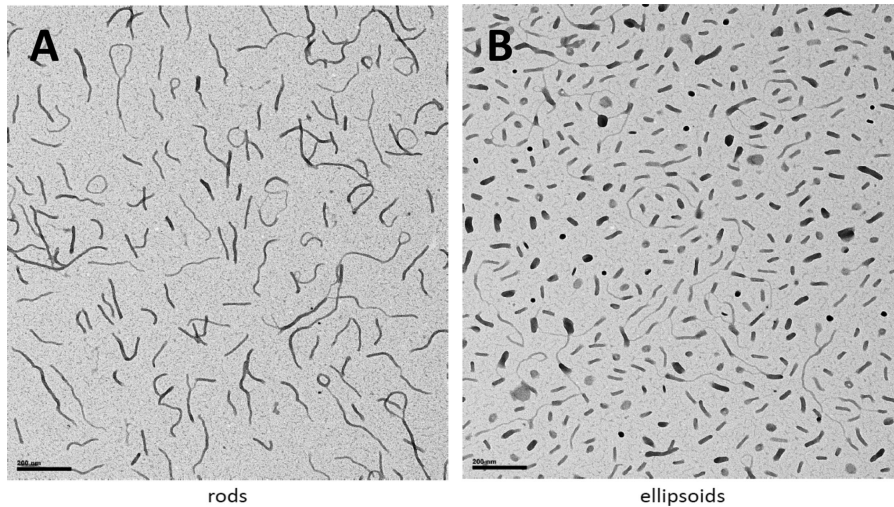


Figure 1. Transmission electron micrographs of rod-shaped (A) and ellipsoid-shaped (B) pEUL DNA NPs manufactured for the rabbit studies. The black bar scale in each photo represents 200 nm.

mixed model for repeated measures, including treatment, visit, and treatment-by-visit interaction as fixed effects, and baseline IOP as a covariate and assuming a compound symmetry covariance matrix. ERG data were analyzed using a one-way analysis of variance (ANOVA) model with treatment group as the fixed effect with Bonferroni's multiple comparison tests to assess statistical significance between groups. Commercially available software (SAS 9.4; SAS Institute, Cary, NC, USA) was used for performing statistical analyses. Luciferase data were analyzed using a one-way ANOVA with Bonferroni's multiple comparison tests between groups using commercially available software (Prism; GraphPad Software, San Diego, CA, USA). Results were considered significant at an α level of 0.05.

Results

Luciferase-DNPs Were Stable in Saline

All DNPs manufactured for the rabbit studies were suspended in normal saline, and these were evaluated using a panel of quality control assays that met all internal specifications. The transmission electron micrographs of the NPs showed the size and shape of the rod and ellipsoidal DNPs (Fig. 1). Based on the 5.3-kb size of the pEUL plasmid, the rod NPs had a diameter of 8 to 11 nm and a length of about 185 nm, and the ellipsoid NPs had a minor diameter of approximately 22 nm and a major diameter of about 50 nm.⁹ Furthermore, the rod and ellipsoid DNPs scattered light according to Rayleigh's law, with a reduction of observed absorbance falling to the fourth power of the incident wavelength, a property that occurs when scattering foci

are small compared to the incident wavelength. The slopes of the turbidity plots were -4.68 for rod DNPs and -4.20 for ellipsoid DNPs. A sedimentation analysis showed that the DNPs did not sediment in saline ($\sim 2\%$ sedimentation) as the ratio of DNA concentration in supernatant to presedimentation (A260 of the supernatant divided by the A260 value of the starting material) was ≥ 0.98 . The endotoxin levels were low (rod-shaped DNPs, 0.40 EU/mg; ellipsoid-shaped DNPs, 2.04 EU/mg).

Suprachoroidal DNPs Exhibited Acceptable Ocular Tolerability in Rabbits

All animals remained healthy during the study, including normal activity, eating, urinations, and defecations. Overt ocular discomfort was not observed. All animals exhibited normal body weight gain over the short duration of this study.

Ocular Examinations

At baseline, no significant ocular abnormalities were noted in the animals prior to the injections. On day 1, most animals that underwent SC injections had mean total ocular examination scores (Hackett and McDonald ocular grading system) of 0 to 2. Typical findings within groups injected suprachoroidally were conjunctival redness and congestion or chemosis in the injected eye. One animal injected with rod-shaped DNPs (SC) was noted to have a posterior cortical cataract, and the retina appeared hazy 24 hours postdose. Animals injected subretinally had statistically higher ($P < 0.009$) mean ocular examination scores of 2 to 3. Typical findings within groups injected subretinally were conjunctival redness, congestion, and

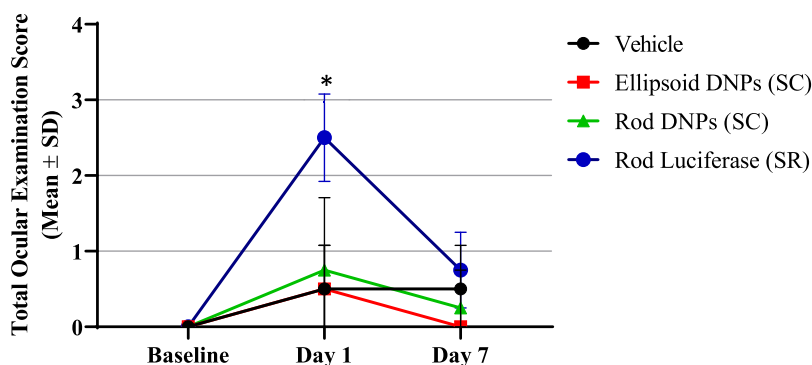


Figure 2. Total ocular exam scores over time. Ocular exams involved conjunctival redness/congestion, chemosis, discharge, corneal opacity, cornea pannus, aqueous flare, pupillary light reflex, cellular flare, lens, ocular fundus, vitreous body, optic nerve head, retinal vasculature and choroidal pathology via slit-lamp, direct and indirect ophthalmoscope, and ocular fundus photography. Ocular examination (OE) scores were comparably low (0–1) for suprachoroidally administered DNP (rod and ellipsoid shape) and control (saline-injected) eyes. OE scores were significantly higher ($P = 0.001$) for subretinally administered DNP (rod shape) on day 1 and similar on day 7 compared to untreated eyes.

chemosis of the injected eye. On day 7, most animals that underwent either SC injections or SR injections had a mean total ocular examination score of 0 to 1. Typical findings within these groups were conjunctival redness. [Figure 2](#) shows the mean total ocular examination scores over time.

Tonometry

At baseline, the IOPs were normal and within range for the age and sex of the animals on study (16.6 ± 2.57 mm Hg). On day 1, a statistically nonsignificant mild increase in IOP in the dosed (left) eyes was noted across all groups except eyes that received SR injections ($P < 0.03$). The undosed (right) eyes across all groups had normal IOPs compared to baseline. On day 7, the IOP returned to the baseline measurements in all injected eyes across groups. [Figure 3](#) shows charts of the IOP from dosed (left) eyes ([Fig. 3A](#)) and undosed (right) eyes ([Fig. 3B](#)) over time.

ERG

At baseline, all animals had normal photopic and scotopic b-wave amplitudes at the initial examination. Seven days postinjection, all animals had mean scotopic b-wave amplitudes similar to corresponding baseline values, albeit at a slightly lower amplitude for vehicle-treated or rod-shaped DNP via SC injection. However, the values overall were consistent with baseline values, with no statistically significant difference among injected animals. Seven days postinjection, all animals had mean photopic b-wave amplitudes similar to corresponding baseline values, with no statistically significant difference among injected animals in the amplitudes of scotopic wave ([Fig. 4A](#)) and

photopic waves ([Fig. 4B](#)). Although considerable inter-subject variability in a-wave amplitudes was measured, no statistically significant decline in a-wave amplitude was observed between baseline (predose) and day 7 postdose time points for all groups tested.

OCT Imaging

OCT images taken at the baseline showed normal retina morphology ([Fig. 5A](#)). On day 1 postinjection, OCT images showed opening and expansion of the SCS without any apparent morphologic changes to the retina immediately after the SC injection. The spread of the DNP injectate was circumferential and posterior, extending to the optic nerve ([Fig. 5B](#)). Images taken 1 month after the SC injections ([Fig. 5C](#)) show complete closure of the SCS.

Histology

Ellipsoid DNP after SC injection. One of four dosed left eyes (OS) examined had no observed signs of intraocular inflammation or toxicity. Two dosed eyes had mild or moderate periocular inflammation (mononuclear cell infiltrate) and in choroid near the sclera. One eye had mild, multifocal areas of mononuclear infiltration, but no intraocular inflammation or signs of toxicity were observed ([Figs. 6A, 6B](#)).

Rod DNP after SC injection. Two of four dosed eyes examined had no observed signs of inflammation or toxicity ([Figs. 6C, 6D](#)). Expanded suprachoroidal space observed in one dosed eye is likely an artifact of the tissue handling and processing as similar observations were made in undosed eyes.

Rod DNP after SR injection. One of four treated eyes had no observed signs of inflammation or toxic-

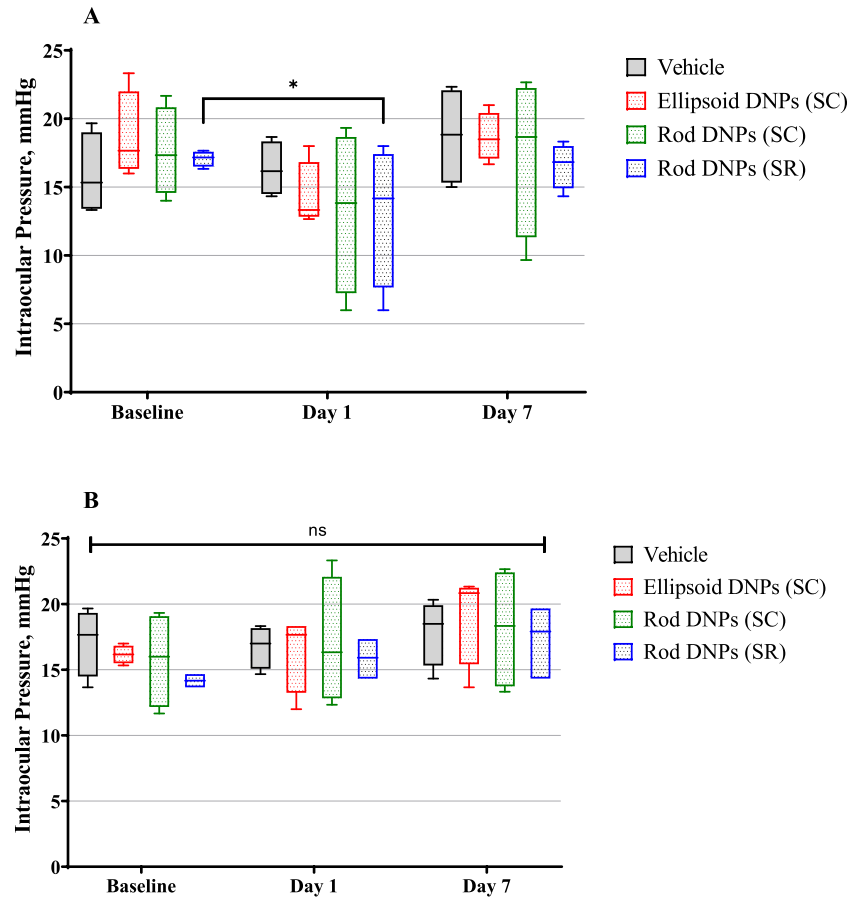


Figure 3. Intraocular pressure (mmHg) from dosed (left) eyes (A) and undosed (right) eyes (B) over time. IOP was measured in triplicate per eye per time point. Mean IOP values were within the normal variability of measurements for all groups except on day 1, when rod-shaped DNPs were administered subretinally ($P = 0.0159$). No statistical difference was observed in mean IOP values among all different groups in the untreated eyes or saline-treated eyes.

ity. Three eyes had signs of mild to moderate retinal inflammation or degeneration, including two eyes that had a focal area of retinitis and retinal separation, with a moderate area of retinal degeneration superior to the optic nerve, and one eye had moderate to severe retinal and subretinal inflammation at site of the SR injection superior to optic nerve (Figs. 6E, 6F).

Comparable Chorioretinal Transfection Observed after SC and SR Delivery of DNPs

Luciferase Activity in RPE-Choroid and Retina

Eyes that received SC DNPs (both rod and ellipsoid shaped) and SR DNPs (rod shaped) exhibited significantly higher (1000-fold, one-way ANOVA, $P < 0.0001$) luciferase activity in the choroid-RPE (Fig. 7A) and in the retina (Fig. 7B) compared to untreated eyes. Eyes administered saline by SC injection had identical low levels of luciferase activity as untreated eyes, which was considered as background signal/noise for

the luciferase activity assay. Transfection in the RPE-choroid was approximately 10-fold higher than that in the retina in animals administered DNPs. In the RPE-choroid or retina, no statistically significant differences were observed between rod- and ellipsoid-shaped DNPs administered suprachoroidally. One of the four samples in the positive control SR group showed no activity in either the RPE-choroid or the retina. In contrast, the SC dosed eyes showed tight clustering of positive activities. Interestingly, the mean luciferase activity in ocular tissues was comparable after SC and SR administrations of DNPs, except for SC ellipsoid DNPs in the choroid, which were higher than SR rod DNPs (Bonferroni $P < 0.05$).

Discussion

Retinal gene delivery is most commonly delivered via SR administration and in some cases via IVT

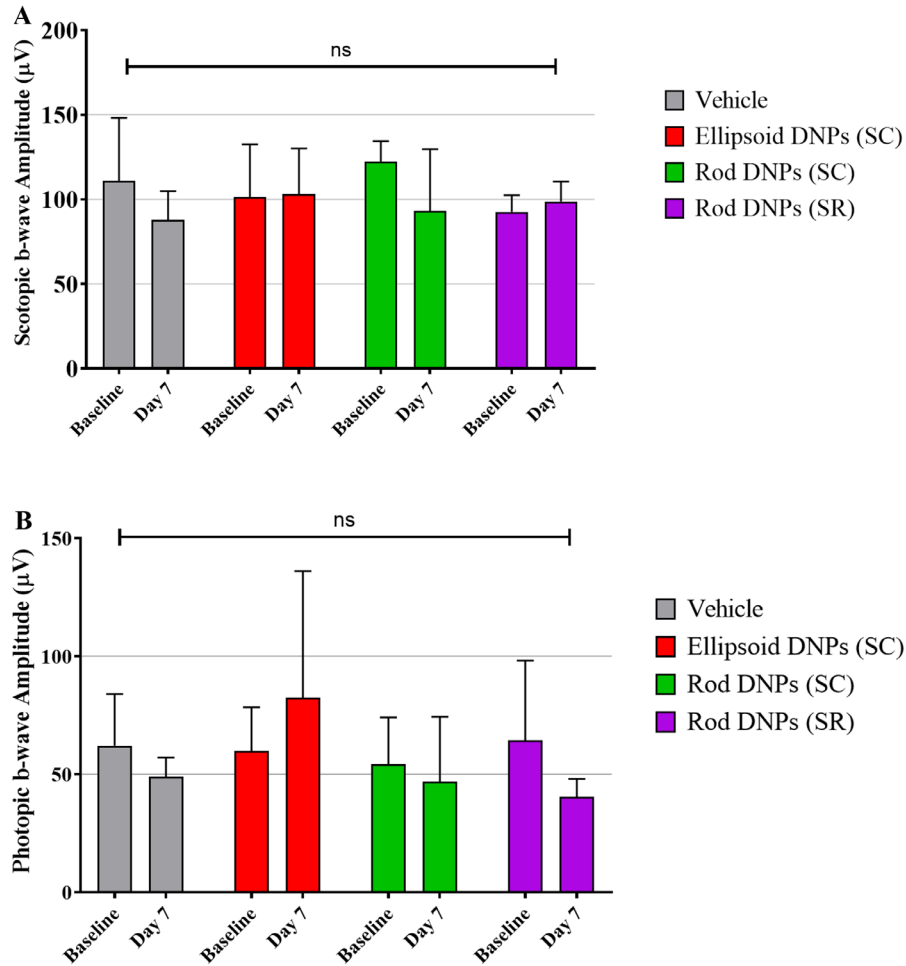


Figure 4. Average scotopic b-wave amplitude (**A**) and photopic b-wave amplitude (**B**) over time. No statistically significant difference was observed among various groups analyzed ($p = ns$; a one-way ANOVA model with treatment group as the fixed effect with Bonferroni's multiple comparison tests to assess statistical significance between groups).

administration. While safety and efficacy of SR and IVT gene delivery have been supported in multiple clinic trials, these delivery routes have limitations. Suprachoroidal gene delivery may offer potential advantages over SR and IVT routes.^{29,30,33} Unlike SR delivery, SC delivery via an office-based microneedle technique eliminates the need for general or retrobulbar anesthesia in an operating room; avoids pars plana vitrectomy with associated complications of cataract, retinal tear, or retinal detachment; and may overcome risks associated with creation of a retinotomy and focal retinal detachment, including acute photoreceptor/RPE injury, hemorrhage, and macular hole, as well as late foveal atrophy. The greater surface area coverage of the posterior segment after SC administration compared to focal SR injection may aid transfection of peripheral retina. The success of intravitreally delivered AAV vector-based gene delivery is limited due to the potential immune response and limited bioavailability

in the photoreceptor and RPE cells due to the presence of the internal limiting membrane.^{25–27} Unlike IVT administration, SC administration is not hindered by the internal limiting membrane; however, the vector must pass through the choroid and Bruch's membrane to reach the targeted retinal layers.

Although the safety and efficacy of AAV vector-based gene therapy platforms have been supported in multiple clinic trials, its limited payload capacity restricts delivery of large genes (>5 kb) such as ABCA4 and USH2A. Additionally, potential risks of host immune and inflammatory responses, manufacturing complexity, and high cost of viral vector-based gene therapy necessitate the development of alternative vectors. The need for a nonviral-based retina gene therapy is further underscored by less than satisfactory and controversial results from the alternative AAV-based approaches that claim to overcome the limited cargo capacity of AAVs.^{39–42}

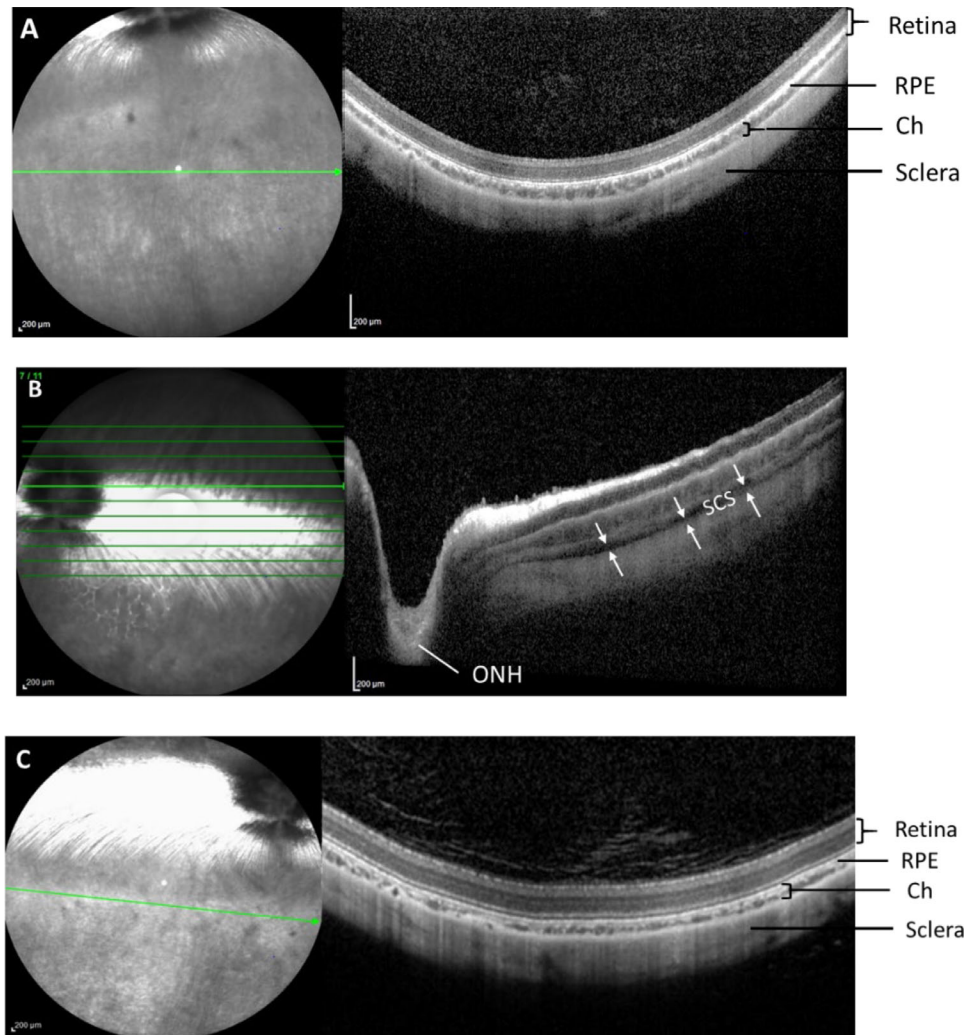


Figure 5. Representative optical coherent tomography images of rabbit eyes at baseline (A), immediately after SC injection on the day of dosing (B), and on day 30 postinjection (C). Double arrows indicate expansion of suprachoroidal space. ch, choroid; ONH, optic nerve head; ret, retina; s, sclera; SCS, suprachoroidal space. Images from the same quadrant of the same eye have been selected for longitudinal assessment.

DNP-based nonviral gene delivery can potentially address IRDs involving genes beyond the carrying capacity of AAV platforms (>5 kb).⁹ Additionally, relatively low immunogenic potential of DNPs potentiates a higher and/or repeat dosing paradigm that may be necessary for the treatment of both chronic inherited diseases and multifactorial acquired conditions, such as AMD, DR, DME, and GA.³⁰ Historically, lower transfection efficiency has been reported for the nonviral-based gene therapy approaches in comparison to viral-based gene therapy. Since repeated SR administration via PPV and retinotomy incurs increased risk, repeat office-based SC administration of DNPs may serve a role. Consequently, we imaged the SCS and evaluated ocular tolerability and transfectability of DNPs after microneedle-based SC administration, in comparison to SR administration.

This research work, for the first time, demonstrates that the microneedle-based SC administration of DNPs was generally tolerable and effectively transfected chorioretinal tissues in rabbits. Most important, SC and SR administration of DNPs resulted in comparable luciferase activity in retina and RPE-choroid. The reported trend for similar transgene expression after subretinal and suprachoroidal administration is well aligned with findings by Shen et al.,³⁰ who reported widespread retinal gene expression in rat eyes after suprachoroidal administration of biodegradable poly- β -ester amine (PBEA) nanoparticles. Significantly higher luciferase activity in the RPE-choroid than in the retina after the SC administration of DNPs suggests a concentration gradient and possibly loss of injected DNPs from the SC space, resulting in a lower number of DNPs available in the inner retina. While

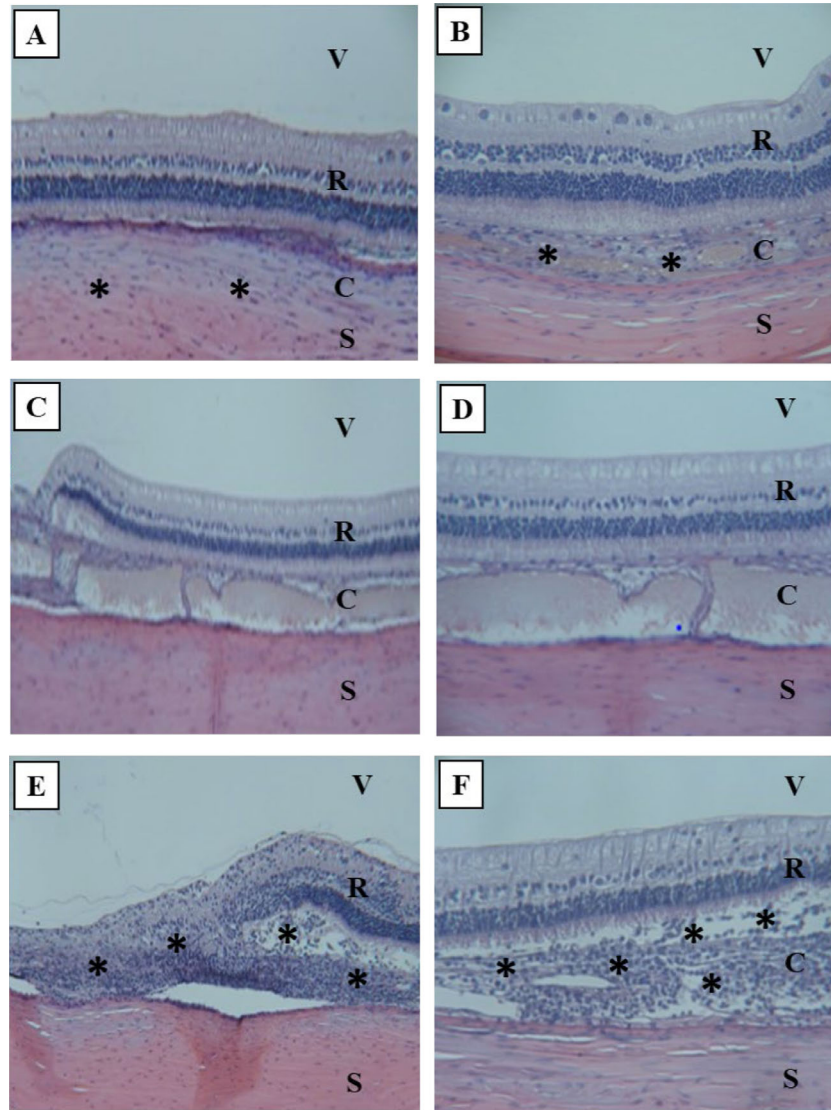


Figure 6. Representative histology images (hematoxylin and eosin stains) of rabbit eyes on day 7 postdose. **(A)** SC ellipsoid DNP (100 \times): No intraocular inflammation. Mild to moderate infiltration of mononuclear cells noted in choroid near sclera. **(B)** SC ellipsoid DNP (400 \times): Mild, multifocal areas of choroidal thickening, mononuclear inflammation; no intraocular inflammation visible. **(C)** SC rod DNP (200 \times): No intraocular inflammation. **(D)** SC rod DNP (400 \times): Expanded suprachoroidal space containing *tan* material (likely artifact). No inflammation or degeneration of adjacent tissue visible. **(E)** SR rod DNP (400 \times): Focal area of retinitis and retinal separation, with a moderate area of retinal degeneration superior to the optic nerve. **(F)** SR rod DNP (600 \times): Moderate to severe retinal and subretinal inflammation at site of SR injection superior to optic nerve. *Asterisks* represent infiltrated mononuclear cells. C, choroid; R, retina; S, sclera; V, vitreous humor.

this ocular distribution needs to be further studied, the SC dosing could be well suited for the treatment of choroidal or RPE disorders.

Given that the endpoint is luciferase activity, the use of a scrambled or nonluciferase transgene as a control group should be identical to the saline control group, with no luciferase protein being produced. Consequently, untreated or saline-treated eyes as control groups were employed to establish baseline and background signal (“noise”) for the luciferase detection assay. Background signal was indeed detected in

control groups, which allowed more accurate comparison of treatment versus control groups. In addition, the eyes that underwent subretinal administration of DNP served as additional controls, for comparison to those eyes that underwent suprachoroidal administration of DNP.

Compared to SC administration, the variability in luciferase activity was higher with the SR administration of DNP. This could be due to the invasive and intricate SR injection procedure, which may have resulted in suboptimal delivery of dosing formulation.

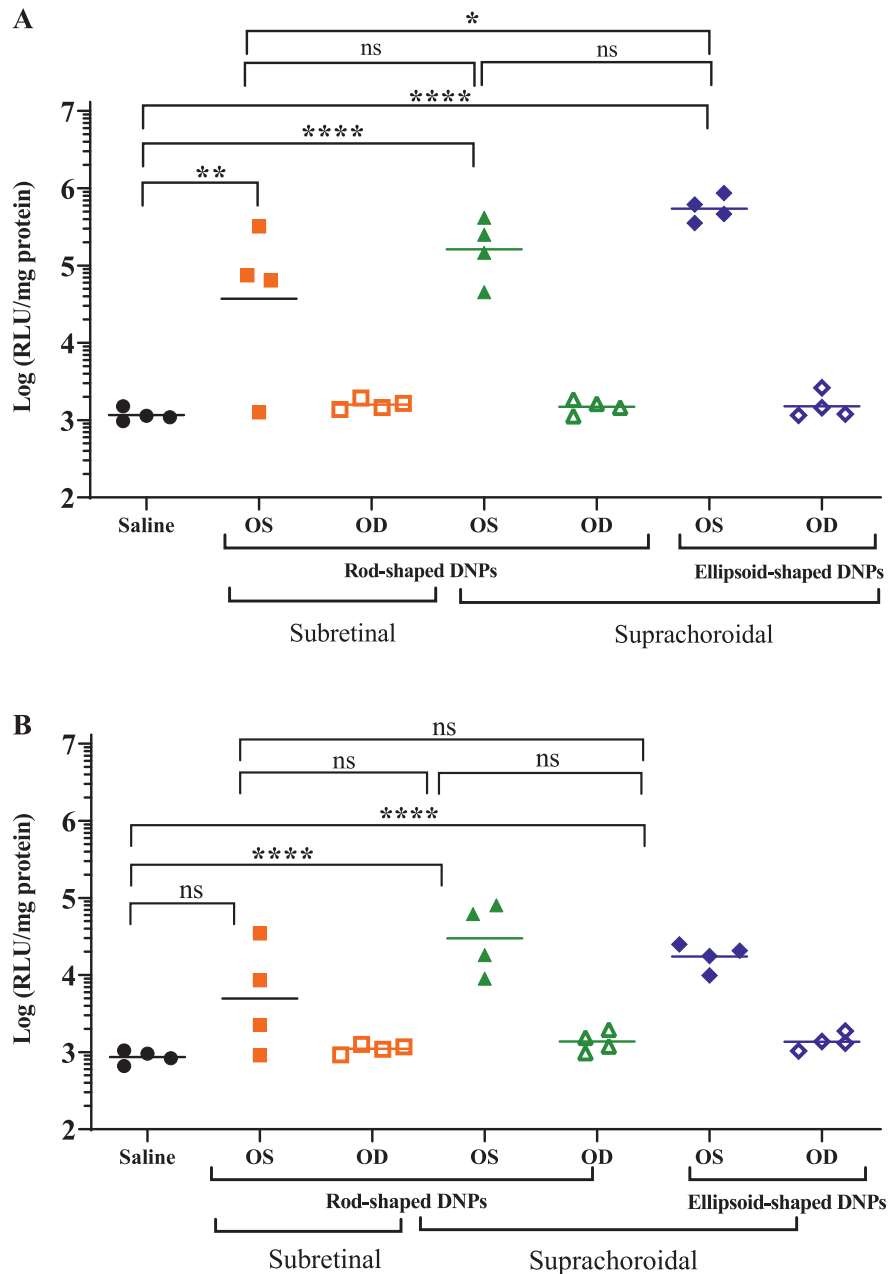


Figure 7. Luciferase activity in the RPE-choroid (**A**) and retina (**B**) of rabbit eyes dosed DNPs either subretinally (SR) with rod-shaped DNPs or suprachoroidally with both rod- and ellipsoid-shaped DNPs. Undosed eyes and saline-injected eyes were negative controls. One-way ANOVA with Bonferroni's multiple comparison test (GraphPad Prism). * $P < 0.05$, ** $P < 0.01$, *** $P < 0.001$, **** $P < 0.0001$. ns, nonsignificant.

In contrast, consistent luciferase activity was observed after the less invasive SC administration. More studies with larger sample sizes are further warranted.

We believe that small size, neutral charge, and nucleolin-mediated nondegradative intracellular translocation may help DNPs to overcome the ocular transport barriers such as choroid, Bruch's membrane, and RPE. Moreover, in contrast to normal ocular anatomy in healthy rabbits in this study, potentially compromised integrity of an anatomic barrier such as

RPE and Bruch's membrane in diseases or conditions in humans may result in paracellular translocation of DNPs across these barriers. In addition, a high concentration gradient of injected DNPs would result in efficient transport and cellular uptake of DNPs in target tissues, as shown in this proof-of-concept study.

The small size of DNPs (~20 nm) may enable diffusion of DNPs through the meshwork of collagen matrix in the choroid and Bruch's membrane. Effective transfection of inner retina and RPE has been

demonstrated via polymeric nanoparticles (~200 nm) and AAV vectors (~25 nm) after SC administration.^{29,30} Moreover, the systemic clearance of DNPs is restricted due to a smaller pore size (~6 nm) of choriocapillaris.⁴³ The neutral surface charge of DNPs may avoid nonspecific interactions with negatively charged cell surface during diffusion from the site of administration (SCS) to the target tissues, RPE, and retina.

Transport across cell membrane is a barrier for nonviral-based nanoparticles. Cellular uptake of DNPs has shown to occur via raft-mediated endocytosis and pinocytosis. DNPs directly bind to nucleolin, a surface protein involved in nucleocytoplasmic transport.^{44,45} Nucleolin has shown to be expressed in all cell layers of mouse retina.⁴⁶ The DNP-nucleolin complex is then endocytosed into cytoplasm via lipid-raft-mediated endocytosis and subsequently trafficked along microtubules directly to the nucleus. Nuclear entry then has been suggested to occur via either passive diffusion through nuclear pores or nucleolin-mediated translocation.^{16,47} This unique cellular uptake and cytoplasmic trafficking mechanism avoids damage to the plasmid DNA cargo in the cytosol and acidic endosome environment and directly transports the cargo to the nucleus, where gene expression occurs.

Once inside the nucleus, the release of plasmid DNA from the compacted DNPs occurs via decompaction of DNA and the polylysine chain in the nucleus via nuclear enzymes (histone methylases, phosphatases) that catalyze polylysine and weaken electrostatic interactions between oppositely charged DNA and polylysine chains. In vitro cell culture studies with analogous DNPs indicate that after nuclear entry, DNPs release biologically active naked DNA in a time course—and dose-dependent manner that is identical to naked DNA.³⁴ Gene transfer and transgene expression of compacted DNA are therefore shown to be quick and efficient.

The potential of SC-delivered AAV and nonviral vectors has been recently assessed. Ding et al.²⁹ demonstrated that AAV8 vector-based SC gene transfer produces widespread ocular transgene expression. Similarly, Yiu et al.³³ demonstrated that SC injection of AAV8-enhanced green fluorescent protein (eGFP) resulted in widespread peripheral transient transgene expression in RPE. Recently, Shen et al.³⁰ reported effective delivery of biodegradable PBEA nanoparticles via suprachoroidal injections in rats using a freehand injection technique. These authors demonstrated successful and widespread transfection of RPE and outer retina cells using a reporter gene and were able to produce efficacious levels of anti-vascular endothelial growth factor (VEGF) proteins in rat eyes. Consequently, a similar distribution might be

expected with DNPs administered suprachoroidally using a microneedle technique, which is supported by findings from our OCT imaging study. The reported trend for similar transgene expression after subretinal and suprachoroidal administration is well aligned with our findings. Results from our rabbit studies further validate the potential of nonviral-based gene delivery to chorioretina via suprachoroidal administration.

Safety and transfection efficiency of other nonviral nanoparticles such as cationic liposomes, polylactic acid (PLA), and polylactic-co-glycolic acid (PLGA) nanoparticles have been assessed for their safety and efficacy of ocular gene transfer, including for glaucoma therapy.^{10,48–50} Subretinal injections of the cationic liposomes have been shown to transfect photoreceptors and RPE cells; however, significant toxicity to photoreceptor cells, even at low concentrations, was observed.⁵¹ Poly-L-lysine-lipoamino acid and polyethylenimine-based dendrimers have shown to transfect RPE cells and retinal ganglion cells after intravitreal delivery,^{52,53} but compared to DNPs, their inherently high cytotoxicity and more complex synthesis process limit the commercial application of dendrimers as nonviral vectors.⁵⁴

Intravitreal delivery of PLA NPs encapsulating fluorescence marker (Rh-6G or Nile red) into rat eyes has been shown to effectively deliver their cargo, assessed via confocal microscopy, fluorescence microscopy, and immunohistochemistry, to the retina and RPE within 24 hours.⁵⁵ Intravitreal delivery of the PLGA NPs into rats with laser-induced choroidal neovascularization (CNV) resulted in eGFP expression in both photoreceptors and RPE at 3 days postinjection, and rats exhibited significantly reduced CNV lesion sizes on day 14 compared to control.⁵⁶ These nanoparticles have not been tested after suprachoroidal delivery. Although no head-to-head comparison can be made due to difference in in vivo species, design of plasmids, and types of reporter and transgenes expressed in different studies, further side-by-side studies comparing safety and efficiency of two or more nonviral vectors after SC administration are warranted.

The shape of the DNPs can be controlled and modulated by formulation design, including the salt counterion of the lysine peptide epsilon amino groups at the time of DNA compaction. An acetate counterion results in DNP rod formation, whereas trifluoroacetate produces DNP ellipsoids.⁹ Since the retina has a complex cellular architecture, it is conceivable that differences in diffusion between rod and ellipsoid DNPs may affect transfection efficiencies in different retinal cell lineages. The shape of DNPs has shown to exhibit a different transfection pattern between

ocular cell types. After SR administration, rod-shaped DNPs have been shown to effectively transfect both RPE and photoreceptor cells, while ellipsoid-shaped DNPs transfected RPE cells. Intravitreal administration of ellipsoid-shaped DNPs resulted in nearly fivefold higher eGFP expression levels in retina than that from rod-shaped DNPs.⁵⁷ In a nonocular indication, cystic fibrosis, only rod-shaped DNPs and not ellipsoid-shaped DNPs exhibited robust luciferase activity in lungs after intramuscular administration.⁵⁸ Rod-shaped DNPs but not ellipsoid-shaped DNPs have been shown to transfect striated muscle cells in mice.⁵⁹ The effect of DNP shape has not been evaluated after suprachoroidal administration. Therefore, we aimed to assess transfection efficiency of rod and ellipsoid DNPs in rabbits after suprachoroidal administration. In this rabbit study, eyes that underwent suprachoroidal injection of rod-shaped DNPs were compared to eyes that underwent suprachoroidal injection of ellipsoid-shaped DNPs. SC dosing of rod and ellipsoid DNPs did not show statistical differences in their ability to transfect retina or choroid, and there were no differences in their tolerability.

DNPs were generally well tolerated after SC and SR administration with no significant impact on retinal functions assessed by ERG, with no statistically significant decline in either a-wave or b-wave amplitudes between baseline and postdose (day 7) time points for all groups. All rabbits survived the entire duration of study. No general health-related issues were noted. Suprachoroidally administered DNPs elicited no to low-grade ocular inflammation, assessed via clinical ocular examinations. The transient ocular inflammation (score 2–3) on day 1 after SR administration of DNPs trended toward baseline within a week of this acute study. A transient increase in the IOP was observed after SC administration of DNPs that returned to baseline by day 7 (the next time point assessed). The IOP change is likely attributable to the volumetric increase via the injected DNPs into a space of finite volume.⁶⁰ However, it is important to note that the IOP change required no additional treatment and was not deemed to induce any adverse event by study investigators. The observed IOP change is likely to be similar to that clinically observed following an intravitreal injection, a standard of route of ocular administration. Implication of higher-volume and/or multiple suprachoroidal injections of DNPs will be further assessed in future studies in a clinically relevant species.

The OCT images in rabbits confirmed the precise delivery of DNPs into the SCS using a proprietary microneedle system (Clearside microinjector), which could potentiate office-based gene therapy. The reversible expansion of the SCS was observed up to

the optic nerve without apparent morphologic changes to the retina, which supports the potential to treat macular disorders. Previous studies investigated thickness and closure kinetics of the SCS in ex vivo rabbits and guinea pig eyes using cryosection and B-wave ultrasound methods.^{61,62} Our observations align with the previous reports confirming expansion of the SCS and posterior distribution of injectate in the eye. In future, the SC delivery method can be optimized further by using a larger injection volume and multiple injections in different quadrants of the eye.

Histology assessment revealed that DNPs injected in SCS had little signs of intraocular toxicity. Suprachoroidally administered ellipsoid-shaped DNPs, and not rod-shaped DNPs, resulted in mild to moderate infiltration of mononuclear cells in choroid, which could be a typical inflammation response to the injection procedure. In contrast, DNPs injected in SRS displayed signs of ocular toxicity, including disorganization and degeneration of retinal cell layers, and focal areas of retinal detachment with mononuclear cell infiltration in subretinal space and in choroid. Long-term future studies with histologic assessment are warranted.

The DNPs employed in our studies are biodegradable, resulting in typical intracellular by-products of plasmid DNA, nucleotide (lysine), and degraded PEG, all materials known to be benign. These by-products are further expected to be degraded and eliminated via cellular endolysosomal degradation pathways and cellular turnover. Although intracellular biodegradation of DNPs in ocular tissues has not been specifically studied, *in vitro* studies using SY5Y (neuroepithelioma) and HuH-7 (hepatoma) cells provide evidence that DNPs degrade and release biologically active DNA after nuclear entry in a time- and dose-dependent manner.³⁴

In this acute study, we have established proof-of-concept of tolerability and transfection ability of SC-delivered DNPs via measures of functional activity of a reporter gene, but quantification of protein levels was not performed. Instead, functional activity of luciferase was quantified via a luciferase bioluminescence technique, which yields indirect information on gene transfection efficiency and does provide information on the functional biological activity of transcribed luciferase protein. Although the luciferase assay offers advantages of having a low background signal in biological tissues, high sensitivity of detection, and ability to assess production of bioactive protein, the luciferase assay required homogenization of ocular tissue samples, which consequently limited our ability to assess cell-specific expression of luciferase in retina and RPE-choroid. Moreover, as the entire retina or

RPE-choroid was collected as one sample, the regional distribution within the tissue is unknown. Our future studies will focus on quantifying the cellular uptake of DNPs in retinal cells with fluorescent-labeled plasmid using a quantitative multiwell plate-based flow cytometry method.⁶³

The possibility of systemic exposure of DNPs after SC administration cannot be completely ruled out, and hence future studies assessing transfection of nonocular tissues are warranted. In a preclinical biodistribution study, DNPs have been detected in the bloodstream shortly after intranasal administration that were then degraded within a few hours.¹⁴ No significant transfection was seen in other organs in animals. Konstan et al.¹² reported no DNP-related systemic adverse events (expected or unexpected) in humans after lung delivery. The potential risk of systemic exposure of DNPs after SC administration and subsequent transgene expression in extraocular tissues will be evaluated in future studies.

To establish further clinical applicability of this proof-of-concept study, long-term expression of therapeutic transgene and assessment of its biologic activity are highly warranted. Our future studies will assess long-term safety of SC-delivered DNPs via chronic single- and repeat-dose toxicity studies in a clinically relevant nonhuman primate model.

Conclusions

Suprachoroidal administration of DNPs via a microneedle technique resulted in reversible opening of the SCS circumferentially and posteriorly, with transfection of chorioretinal tissues in rabbits comparable to SR administration. Further studies are warranted to assess long-term safety, efficiency, and durability of SC-administered DNPs. Acceptable ocular tolerability and comparable transfectability of suprachoroidally and subretinally administered DNPs in this proof-of-platform study, combined with the potential of nonviral vector-based gene therapy, may pave a path to an office-based ocular gene therapy.

Acknowledgments

The authors thank Barry Kapik (Clearside Biomedical, Inc.) for his help with the statistical analysis of the data and Glenn Noronha, Donna Taraborelli, and Jesse Yu (former employees of Clearside Biomedical) for their contribution in planning and acquisition of the study data for initial cohort of animals.

Disclosure: **V.S. Kansara**, Clearside Biomedical, Inc. (E, F); **M. Cooper**, Copernicus Therapeutics (E, F); **O. Sesenoglu-Laird**, Copernicus Therapeutics (E, F); **L. Muya**, Clearside Biomedical, Inc. (E, F); **R. Moen**, Copernicus Therapeutics (E, F); **T.A. Ciulla**, Clearside Biomedical, Inc. (E, F)

References

1. US Food and Drug Administration. FDA approves novel gene therapy to treat patients with a rare form of inherited vision loss. Available at: <https://www.fda.gov/news-events/press-announcements/fda-approves-novel-gene-therapy-treat-patients-rare-form-inherited-vision-loss>. Accessed June 3, 2020.
2. Trapani I, Auricchio A. Has retinal gene therapy come of age? From bench to bedside and back to bench. *Hum Mol Genet.* 2019;28(R1):R108–R118.
3. Moore NA, Morral N, Ciulla TA, Bracha P. Gene therapy for inherited retinal and optic nerve degenerations. *Expert Opin Biol Ther.* 2018;18(1):37–49.
4. Seidman C, Kiss S. Gene therapy: the next frontier for treatment of acquired and inherited ocular disorders. *Retina Today.* 2015;69–71.
5. Moore NA, Bracha P, Hussain RM, Morral N, Ciulla TA. Gene therapy for age-related macular degeneration. *Expert Opin Biol Ther.* 2017;17(10):1235–1244.
6. Campochiaro PA, Nguyen QD, Shah SM, et al. Adenoviral vector-delivered pigment epithelium-derived factor for neovascular age-related macular degeneration: results of a phase I clinical trial. *Hum Gene Ther.* 2006;17(2):167–176.
7. Constable IJ, Lai C-M, Magno AL, et al. Gene therapy in neovascular age-related macular degeneration: three-year follow-up of a phase 1 randomized dose escalation trial. *Am J Ophthalmol.* 2017;177:150–158.
8. Adverum Biotechnologies. Adverum Biotechnologies reports new interim data from cohorts 1 and 2 of OPTIC phase 1 trial of ADV-022 intravitreal gene therapy for wet AMD at Angiogenesis, Exudation and Degeneration 2020. Published June 7, 2020. Available at: <http://investors.adverum.com/news-releases/news-release-details/adverum-biotechnologies-reports-new-interim-data-cohorts-1-and-2>. Accessed June 7, 2020.
9. Fink TL, Klepcyk PJ, Oette SM, et al. Plasmid size up to 20 kbp does not limit effective in vivo lung

- gene transfer using compacted DNA nanoparticles. *Gene Ther.* 2006;13(13):1048–1051.
10. Adijanto J, Naash MI. Nanoparticle-based technologies for retinal gene therapy. *Eur J Pharm Biopharm.* 2015;95(pt B):353–367.
 11. Padegimas L, Kowalczyk TH, Adams S, et al. Optimization of hCFTR lung expression in mice using DNA nanoparticles. *Mol Ther.* 2012;20(1):63–72.
 12. Konstan MW, Davis PB, Wagener JS, et al. Compacted DNA nanoparticles administered to the nasal mucosa of cystic fibrosis subjects are safe and demonstrate partial to complete cystic fibrosis transmembrane regulator reconstitution. *Hum Gene Ther.* 2004;15(12):1255–1269.
 13. Ding X-Q, Quiambao AB, Fitzgerald JB, Cooper MJ, Conley SM, Naash MI. Ocular delivery of compacted DNA-nanoparticles does not elicit toxicity in the mouse retina. *PLoS One.* 2009;4(10):e7410.
 14. Ziady A-G, Gedeon CR, Muhammad O, et al. Minimal toxicity of stabilized compacted DNA nanoparticles in the murine lung. *Mol Ther.* 2003;8(6):948–956.
 15. Yurek DM, Fletcher AM, McShane M, et al. DNA nanoparticles: detection of long-term transgene activity in brain using bioluminescence imaging. *Mol Imaging.* 2011;10(5):327–339.
 16. Walsh M, Tangney M, O'Neill MJ, et al. Evaluation of cellular uptake and gene transfer efficiency of pegylated poly-L-lysine compacted DNA: implications for cancer gene therapy. *Mol Pharm.* 2006;3(6):644–653.
 17. Chen X, Davis PB. Compacted DNA nanoparticles transfect cells by binding to cell surface nucleolin. *Mol Ther.* 2006;13:S152.
 18. Chen X, Davis PB. Intracellular trafficking of DNA nanoparticle and nucleolin antibody. *Mol Ther.* 2007;15:S196.
 19. Cai X, Conley SM, Nash Z, Fliesler SJ, Cooper MJ, Naash MI. Gene delivery to mitotic and postmitotic photoreceptors via compacted DNA nanoparticles results in improved phenotype in a mouse model of retinitis pigmentosa. *FASEB J.* 2010;24(4):1178–1191.
 20. Cai X, Nash Z, Conley SM, Fliesler SJ, Cooper MJ, Naash MI. A partial structural and functional rescue of a retinitis pigmentosa model with compacted DNA nanoparticles. *PLoS One.* 2009;4(4):e5290.
 21. Han Z, Koirala A, Makkia R, Cooper MJ, Naash MI. Direct gene transfer with compacted DNA nanoparticles in retinal pigment epithelial cells: expression, repeat delivery and lack of toxicity. *Nanomedicine.* 2012;7(4):521–539.
 22. Koirala A, Makkia RS, Cooper MJ, Naash MI. Nanoparticle-mediated gene transfer specific to retinal pigment epithelial cells. *Biomaterials.* 2011;32(35):9483–9493.
 23. Han Z, Conley SM, Makkia R, Guo J, Cooper MJ, Naash MI. Comparative analysis of DNA nanoparticles and AAVs for ocular gene delivery. *PLoS One.* 2012;7(12):e52189.
 24. Kay C. Retinal gene therapies in clinical trials—a proliferation of clinical trials means hope for patients. *Retina Physician.* 2019;16:36–40.
 25. Cukras C, Wiley HE, Jeffrey BG, et al. Retinal AAV8-RS1 gene therapy for X-linked retinoschisis: initial findings from a phase I/IIa trial by intravitreal delivery. *Mol Ther.* 2018;26(9):2282–2294.
 26. Yang S, Ma S qi, Wan X, et al. Long-term outcomes of gene therapy for the treatment of Leber's hereditary optic neuropathy. *EBioMedicine.* 2016;10:258–268.
 27. Reichel FF, Peters T, Wilhelm B, et al. Humoral immune response after intravitreal but not after subretinal AAV8 in primates and patients. *Invest Ophthalmol Vis Sci.* 2018;59(5):1910–1915.
 28. Habot-Wilner Z, Noronha G, Wykoff CC. Suprachoroidally injected pharmacological agents for the treatment of chorio-retinal diseases: a targeted approach. *Acta Ophthalmol.* 2019;97(5):460–472.
 29. Ding K, Shen J, Hafiz Z, et al. AAV8-vectored suprachoroidal gene transfer produces widespread ocular transgene expression. *J Clin Invest.* 2019;129(11):4901–4911.
 30. Shen J, Kim J, Tzeng SY, et al. Suprachoroidal gene transfer with nonviral nanoparticles. *Sci Adv.* 2020;6(27):eaba1606.
 31. Yeh S, Khurana RN, Shah M, et al. Efficacy and safety of suprachoroidal CLS-TA for macular edema secondary to noninfectious uveitis: phase 3 randomized trial. *Ophthalmology.* 2020;127(7):948–955.
 32. Kansara V, Muya L, Wan C, Ciulla TA. Suprachoroidal delivery of viral and nonviral gene therapy for retinal diseases. *J Ocul Pharmacol Ther.* 2020;36(6):384–392.
 33. Yiu G, Chung SH, Mollhoff IN, et al. Suprachoroidal and subretinal injections of AAV using transscleral microneedles for retinal gene delivery in nonhuman primates. *Mol Ther Methods Clin Dev.* 2020;16:179–191.
 34. Liu G, Li D, Pasumarthy MK, et al. Nanoparticles of compacted DNA transfect postmitotic cells. *J Biol Chem.* 2003;278(35):32578–32586.
 35. Ziady A-G, Gedeon CR, Miller T, et al. Transfection of airway epithelium by stable PEGylated

- poly-L-lysine DNA nanoparticles in vivo. *Mol Ther.* 2003;8(6):936–947.
36. del Amo EM, Urtti A. Rabbit as an animal model for intravitreal pharmacokinetics: clinical predictability and quality of the published data. *Exp Eye Res.* 2015;137:111–124.
 37. Peden MC, Min J, Meyers C, et al. Ab-externo AAV-mediated gene delivery to the suprachoroidal space using a 250 micron flexible microcatheter. *PLoS One.* 2011;6(2):e17140.
 38. Hackett RB, McDonald TO. Ophthalmic toxicology and assessing ocular irritation. In: Marzulli FN, Maibach HI, eds. *Derma Toxicology*. 5th ed. Washington, DC: Hemisphere; 1996;299–305:557–566.
 39. Dyka FM, Boye SL, Chiodo VA, Hauswirth WW, Boye SE. Dual adeno-associated virus vectors result in efficient in vitro and in vivo expression of an oversized gene, MYO7A. *Hum Gene Ther Methods.* 2014;25(2):166–177.
 40. McClements ME, Barnard AR, Singh MS, et al. An AAV dual vector strategy ameliorates the Stargardt phenotype in adult *Abca4*(*-/-*) mice. *Hum Gene Ther.* 2019;30(5):590–600.
 41. Carvalho LS, Turunen HT, Wassmer SJ, et al. Evaluating efficiencies of dual AAV approaches for retinal targeting. *Front Neurosci.* 2017;11:503.
 42. Maddalena A, Tornabene P, Tiberi P, et al. Triple vectors expand AAV transfer capacity in the retina. *Mol Ther.* 2018;26(2):524–541.
 43. Sarin H. Physiologic upper limits of pore size of different blood capillary types and another perspective on the dual pore theory of microvascular permeability. *J Angiogenesis Res.* 2010;2(1):1–19.
 44. Ginisty H, Sicard H, Roger B, Bouvet P. Structure and functions of nucleolin. *J Cell Sci.* 1999;112(6):761–772.
 45. Chen X, Shank S, Davis PB, Ziady AG. Nucleolin-mediated cellular trafficking of DNA nanoparticle is lipid raft and microtubule dependent and can be modulated by glucocorticoid. *Mol Ther.* 2011;19(1):93–102.
 46. Conley SM, Naash MI. Nanoparticles for retinal gene therapy. *Prog Retin Eye Res.* 2010;29(5):376–397.
 47. Chen X, Kube DM, Cooper MJ, Davis PB. Cell surface nucleolin serves as receptor for DNA nanoparticles composed of pegylated polylysine and DNA. *Mol Ther.* 2008;16(2):333–342.
 48. Luo L-J, Nguyen DD, Lai J-Y. Dually functional hollow ceria nanoparticle platform for intraocular drug delivery: a push beyond the limits of static and dynamic ocular barriers toward glaucoma therapy. *Biomaterials.* 2020;243:119961.
 49. Lai J-Y, Luo L-J, Nguyen DD. Multifunctional glutathione-dependent hydrogel eye drops with enhanced drug bioavailability for glaucoma therapy. *Chem Eng J.* 2020;402:126190.
 50. Nguyen DD, Luo L-J, Lai J-Y. Effects of shell thickness of hollow poly(lactic acid) nanoparticles on sustained drug delivery for pharmacological treatment of glaucoma. *Acta Biomater.* 2020;111:302–315.
 51. Masuda I, Matsuo T, Yasuda T, Matsuo N. Gene transfer with liposomes to the intraocular tissues by different routes of administration. *Investig Ophthalmol Vis Sci.* 1996;37(9):1914–1920.
 52. Marano RJ, Toth I, Wimmer N, Brankov M, Rakoczy PE. Dendrimer delivery of an anti-VEGF oligonucleotide into the eye: a long-term study into inhibition of laser-induced CNV, distribution, uptake and toxicity. *Gene Ther.* 2005;12(21):1544–1550.
 53. Liao H-W, Yau K-W. In vivo gene delivery in the retina using polyethylenimine. *Biotechniques.* 2007;42(3):285–286, 288.
 54. Chaplot SP, Rupenthal ID. Dendrimers for gene delivery—a potential approach for ocular therapy? *J Pharm Pharmacol.* 2014;66(4):542–556.
 55. Bourges J-L, Gautier SE, Delie F, et al. Ocular drug delivery targeting the retina and retinal pigment epithelium using polylactide nanoparticles. *Invest Ophthalmol Vis Sci.* 2003;44(8):3562–3569.
 56. Zhang C, Wang Y-S, Wu H, et al. Inhibitory efficacy of hypoxia-inducible factor 1alpha short hairpin RNA plasmid DNA-loaded poly (D, L-lactide-co-glycolide) nanoparticles on choroidal neovascularization in a laser-induced rat model. *Gene Ther.* 2010;17(3):338–351.
 57. Farjo R, Skaggs J, Quiambao AB, Cooper MJ, Naash MI. Efficient non-viral ocular gene transfer with compacted DNA nanoparticles. *PLoS One.* 2006;1(1):e38.
 58. Cooper MJ. United States Patent 8,017,577. Lyophilizable and enhanced compacted nucleic acids. 2011.
 59. Kowalczyk T, Pasumarthy M, Gedeon C, et al. Type of polylysine counterion influences morphology and biological function of condensed DNA. *Mol Ther.* 2001;3:S359.
 60. Lee JW, Park H, Choi JH, et al. Short-term changes of intraocular pressure and ocular perfusion pressure after intravitreal injection of bevacizumab or ranibizumab. *BMC Ophthalmol.* 2016;16(1):4–10.
 61. Gu B, Liu J, Li X, Ma Q, Shen M, Cheng L. Real-time monitoring of suprachoroidal space (SCS) following SCS injection using ultra-high resolution

- optical coherence tomography in guinea pig eyes. *Invest Ophthalmol Vis Sci.* 2015;56(6):3623–3634.
62. Chiang B, Venugopal N, Grossniklaus HE, Jung JH, Edelhauser HF, Prausnitz MR. Thickness and closure kinetics of the suprachoroidal space following microneedle injection of liquid formulations. *Invest Ophthalmol Vis Sci.* 2017;58(1):555–564.
63. Bishop CJ, Majewski RL, Guiriba T-RM, et al. Quantification of cellular and nuclear uptake rates of polymeric gene delivery nanoparticles and DNA plasmids via flow cytometry. *Acta Biomater.* 2016;37:120–130.